The COST 259 Directional Channel Model Part II: Macrocells

Asplund, Henrik; Alayon Glazunov, Andres; Molisch, Andreas; Pedersen, Klaus I.; Stenbauer, Martin

Published in:
IEEE Transactions on Wireless Communications

DOI:
10.1109/TWC.2006.01118

2006

The COST 259 Directional Channel Model–Part II: Macrocells

Henrik Asplund, *Member, IEEE,* Andrés Alayón Glazunov, *Student Member, IEEE*, Andreas F. Molisch, *Fellow, IEEE,* Klaus I. Pedersen, *Member, IEEE*, and Martin Steinbauer, *Member, IEEE*

***Abstract*— This paper describes the attributes of the COST 259 directional channel model that are applicable for use in the design and implementation of macrocellular mobile and portable radio systems and associated technology. Special care has been taken to model all propagation mechanisms that are currently understood to contribute to the characteristics of practical macrocellular channels and confirm that large scale, small scale, and directional characteristics of implemented models are realistic through their comparison with available measured data. The model that is described makes full use of previously published work, as well as incorporating some new results. It is considered that its implementation should contribute to a tool that can be used for simulations and comparison of different aspects of a large variety of wireless communication systems, including those that exploit the spatial aspects of radio channels, as, for example, through the use of adaptive antenna systems.**

***Index Terms*— Direction of arrival, mobile radio channel, smart antenna.**

I. Introduction

THE COST 259 directional channel model was developed within the European research initiative COST 259 [1] and it is proposed that it be adopted as a new standard model for mobile radio channels. During the development of this model, special emphasis was placed on modeling the directional properties of the channel to allow studies of diversity and adaptive antenna systems. This paper has the objective of describing how the COST 259 model framework described in a companion paper [2] can be used for simulations applicable to the macrocell case, in which base station antennas are mounted above most surrounding rooftops to provide wide area coverage. It is intended that use of the same framework to simulate channel behavior in microcells and picocells will be described in another companion paper [3].

Previous efforts at modeling directional [4]-[14] and non-directional [15]-[30], macrocellular channels have been taken into consideration when designing the model, as well as a wealth of published [31]-[59] and some previously unpublished material on channel measurements. The previously unpublished material includes raw data from directional channel measurements in various macrocellular environments that were performed by the authors. However most of the experimental database was compiled from reports on the analysis and parameterization of propagation measurement results by other researchers who used channel sounders that had a range of different characteristics. The model has been parameterized using measurements in the 0.5-2 GHz frequency range with bandwidths up to 5 MHz. There are indications that the model could be appropriate for higher bandwidths and other frequencies, however until further measurement data are available, this cannot be recommended. The experimental results are from measurements with a variety of antennas with different antenna patterns and polarizations at both the mobile and base stations. A flexible channel model with the ability to reproduce all such results should consider only the medium between the transmitting and receiving antenna, and thus allow combination of the model with arbitrary antennas. The modeling of angular and polarization characteristics of the channel in the current work is based primarily on measurements made specifically for their determination, where the influence of the measurement antennas and equipment has been accounted for.[1] As an example, the measurements used for forming a model of the angular distribution of waves at the mobile station include a validation of the estimation of azimuth and elevation angles under line-of-sight conditions [56]. Similarly, the paper by Lee and Yeh [50], which had the most influence on the polarization model, contains a sensitivity analysis of how the height of the mobile antennas above an automobile roof influences the received power per polarization. It should be noted that contrary to the situation in a practical system, the immediate surroundings of the measurement antennas are usually free from objects, most notable is the absence of a user. The influence of the user, therefore, needs to be included with

Manuscript received May 15, 2001; revised April 18, 2005; accepted October 4, 2005. The associate editor coordinating the review of this letter and approving it for publication was P. Driessen.

H. Asplund is with Ericsson Research, Stockholm, Sweden (e-mail: henrik.asplund@ericsson.com).

A. A. Glazunov was with Ericsson Research. He is now with Lund University, Lund, Sweden (email: andres.alayon@es.lth.se).

A. F. Molisch was with the Institut für Nachrichtentechnik und Höchfrequenztechnik (INTHF) of the TU Wien, Vienna, Austria and with AT&T Labs-Research, Middletown, NJ, USA. He is now with Mitsubishi Electric Research Labs, Cambridge, MA USA, and also at Lund University, Lund, Sweden (e-mail: andreas.molisch@ieee.org).

K. I. Pedersen was with Aalborg University, Denmark. He is now with Nokia Networks, Aalborg, Denmark.

M. Steinbauer was with the INTHF of the TU Wien, Vienna, Austria. He is now with mobilkom, Austria (e-mail: m.steinbauer@mobilkomaustriagroup.com).

Digital Object Identifier 10.1109/TWC.2006.01118

[1]This is not true in general. For instance, most measurements of time dispersion do not consider the influence that the transmitting or receiving antenna has on the results. However, in the experience of the authors, the effect is minor compared to the variance of time dispersion due to variations in the propagation environment.

the characteristics of the mobile antenna that the directional channel model is to be combined with.

A key observation resulting from the analysis of directional wideband measurements in macrocellular environments is that energy is clustered into isolated intervals in delay and in solid angle at the base station (BS) and the mobile station (MS). The clustering is not always distinct in all three dimensions; in particular, at the MS there can be significant overlap between clusters that are clearly distinguishable in delay or angle at the BS. This is a result of the larger angular spread at the MS end of the link, which is caused by the fact that most Interacting Objects (IOs) [2] are in the vicinity of the MS. As time evolves and the MS moves through the environment, the clusters usually stay intact because the evolution of the observable multipath components (MPCs) in delay and in solid angle at the BS is similar within each group. However, given sufficiently high resolution of angles at the MS (or in delay), it becomes evident that a cluster that may look cohesive in the angular domain at the BS actually consists of MPCs with different time evolution of their respective angles (and delays) at the MS. The difference primarily results from the geometry of the trajectory of the MS in relation to the positions of the IOs, but also from the constantly changing set of IOs that influence the channel characteristics.

The minimum resolution needed in MS angle and delay to be able to identify the differences in time-evolution of the MPCs is unknown, although the work in [59] is reported to have resulted in the resolution of all the strongest MPCs using a measurement system with $40^\circ \times 3$ ns resolution. When the resolution capabilities are lower, such as for the systems that the COST 259 DCM primarily will be used for simulating, the individual MPCs received from distinct IOs will not be resolvable. In this situation the channel can be described using a set of multipath groups (MPGs) where each of the MPGs contain the combined energy of several MPCs. The combination of several MPCs into one MPG tends to suppress the individual differences in time evolution.

In the COST 259 DCM, a cluster is defined as a collection of MPGs that are within the same isolated interval in at least one, and possibly more, of the dimensions delay, BS angle and MS angle, and that share the same long-term evolution such that the cluster remains intact over time. It is conjectured that the MPGs within a cluster have no individual differences in their respective long-term evolution. This model assumption represents a deviation from the real-world physics that will cause an increasing error with increasing system bandwidth and angular resolving capabilities at the MS, although for recommended maximum bandwidth of 5 MHz and for mobile stations with just a few antennas the error should be small. The major benefit is a more simple model, in which the number of clusters and their descriptive parameters is limited. Modeling of the clustered nature of the channel is motivated by consideration of the influence the clusters would have on optimizing transmission or reception of energy over the channel. Clustering in the angular domain affects the efficiency of beamforming techniques, while clustering in the delay domain influences the design of receivers or equalizers.

Another important feature of the COST 259 directional channel model is that it incorporates options that allow the statistics of simulated channel variations to change as a result of changes in the general location of the MS. In past simulation models, the statistics of generated channel characteristics remained the same for all time and all simulations were made with the same initial parameter settings. When using past models, therefore, wireless systems must be evaluated under the assumption that variations on each link in the system have the same statistics, and are merely from uncorrelated realizations of the same underlying process.

However, there are two situations, where it is important that realizations of the channel process be generated so as to have different statistical characteristics. The first of these is when algorithms being evaluated by simulation (e.g. a channel estimator or finger tracker in a Rake receiver or algorithms for handover) must be evaluated over time frames that exceed the length of time[2] over which the channel is statistically stationary. The second such situation is that in which there are multiple users sharing the same radio resources, that can interfere with each other. The existence of different statistics associated with variability on links to different users can influence the effectiveness of methods and technology, such as adaptive antennas, to mitigate interference. This can be simulated using the COST 259 DCM.

The COST 259 model is also complete in the sense that it jointly addresses most aspects of the channel, including path loss, fast fading, delay and angular spread, and polarization. This is a prerequisite for the comparison of systems that utilize these properties of the channel in different ways, such as for micro- or macro-diversity, or when adaptive antennas are used, etc. Within the COST 259 model framework, such comparisons are made possible by the fact that a single channel model is available that realistically reflects all the important channel characteristics and associated parameters.

An explanation of the model begins with a definition of what is referred to as a radio environment in the COST 259 model framework, and four such environments are described in Section II. The structure of the double-directional channel impulse response as described in [2] is briefly repeated in Section III, where external and global parameters are also introduced. Section IV reports experimental observations and modeling approaches for each of the global parameters, including the modeling of dynamic variations and correlations among the variations of different parameters. A brief guide to implementing the model in a simulator can be found in Section V. Finally, in Section VI, the degree to which results from application of the model reflect real-world channel characteristics is assessed by comparison of modeling results with results from the analysis of measured data.

II. Macrocellular Radio Environments

As soon as one starts analyzing channel measurements from macrocells it becomes apparent that typical values of parameters like delay spread or angular spread have a wide variation depending on the location of the measurement. By subdividing macrocells into different radio environments like rural areas and cities, it is found that the variation within each

[2]Time evolution is equivalent to motion through space in the COST 259 DCM, since a fixed environment is assumed.

TABLE I
EXTERNAL PARAMETERS

Parameter	Symbol	Valid range	Typical value
Carrier frequency [Hz]	f	150 MHz-2 GHz (GRA,GHT) 800 MHz-2 GHz (GTU,GBU)	
Bandwidth [Hz]	BW	0-5 MHz	
Base station height [m]	h_{BS}	30-200 m (GRA,GHT) 4-50 m (GTU,GBU)	50 m (GBU,GRA,GHT) 30 m (GTU)
Mobile station height [m]	h_{MS}	1-10 m (GRA,GHT) 1-3 m (GTU,GBU)	1.5 m
Base station position [m]	$\overline{r}_{BS}$	Any	
Mobile station position [m]	$\overline{r}_{MS}$ $d = \lvert\overline{r}_{MS} - \overline{r}_{BS}\rvert$	$d < 20$ km (GRA,GHT) $d < 5$ km (GTU,GBU)	$d = 5000$ m (GRA,GHT) $d = 500$ m (GTU,GBU)
Average building height [m]	h_B	8-60 m, $h_B < h_{BS}$	15 m (GTU), 30 m (GBU)
Width of roads [m]	w	Any	$b/2$
Building separation [m]	b	Any	30 m (GTU), 50 m (GBU)
Road orientation with respect to direct path	φ_R	0-90°	45°

subset can be significantly reduced. This is attractive from a modeling viewpoint.

Four macro-cellular radio environments have been characterized in the COST 259 model, and are referred to as Generalized Typical Urban, Generalized Bad Urban, Generalized Rural Area, and Generalized Hilly Terrain[3] environments. They were chosen to coincide with the COST 207 models [15], which became well known to the general public when they were used in the GSM standard [16]. The word "generalized" in the names denotes the fact that the COST 259 radio environments are much more general than those of the COST 207 model. The generalization not only comes from the introduction of the directional domain, but also from the introduction of statistical distributions for several channel parameters. Still, the COST 207 models may be viewed as typical (non-directional) realizations of the COST 259 macrocellular model [63]. The definitions of the macrocell radio environments in the COST 259 model are as follows:

Generalized Typical Urban (GTU):

Cities and towns where the buildings have nearly uniform height and density fall into the Generalized Typical Urban category. Due to the uniformity of the environment, IOs are predominantly found in the local area around the MS, although a few distant groups of IOs could also be influential.

Generalized Bad Urban (GBU):

Cities with distinctly nonuniform building heights or densities belong to the Generalized Bad Urban category. Prime examples are high-rise metropolitan centres and cities with large open areas such as rivers, lakes or parks. Energy received via both local and one or several distant groups of IOs can contribute to the received signal.

Generalized Rural Area (GRA):

The Generalized Rural Area category describes an environment where buildings are few, such as farmlands, fields and forests. IOs in the form of natural objects occasionally act as a source of MPCs at long delays.

[3]As in the COST 207 models, there is no Suburban radio environment. However, it can be easily added by specifying appropriate parameter values.

Generalized Hilly Terrain (GHT):

The Generalized Hilly Terrain environment is like the Generalized Rural Area, but with large height variations such as hills or mountains. This radio environment covers hilly terrain, as well as mountainous and alpine terrain. Diffuse scattering from hillsides or mountains contribute significantly to the channel characteristics.

Each of the radio environments is specified with a set of parameters and models for generating the propagation scenarios described in [2], which are each characterized by a set of MPCs that can locally be regarded as having constant delay, angles of arrival and departure, amplitude, phase and polarization. A propagation scenario is valid over a local area the size of a few wavelengths, where only the phase shift of each MPC due to the relative position within the area needs to be accounted for. The parameters that are associated with each radio environment are called global parameters and will be described in more detail in Section IV.

III. MODEL STRUCTURE

In addition to the global parameters that define a radio environment, some parameters are left to the user of the model to specify. These *external* (user-supplied) parameters for the macro-cell model are summarized in Table I along with the validity ranges of the model. These parameters describe the simulation environment and can, in contrast to some of the global parameters, be easily understood even by someone without a thorough understanding of radiowave propagation. The validity ranges given in the table result from use of the associated path loss models, which have only been verified within this range. All other modeled channel parameters, including delay and angular spread, polarization, clustering etc have only been verified for some values of these parameters, but there are no indications of dependencies on the external parameters with the possible exception of the azimuth spread being dependent on BS antenna height [38].

Following Eq. (4) of [2], the double-directional impulse response of a radio channel is written as a sum of L MPCs

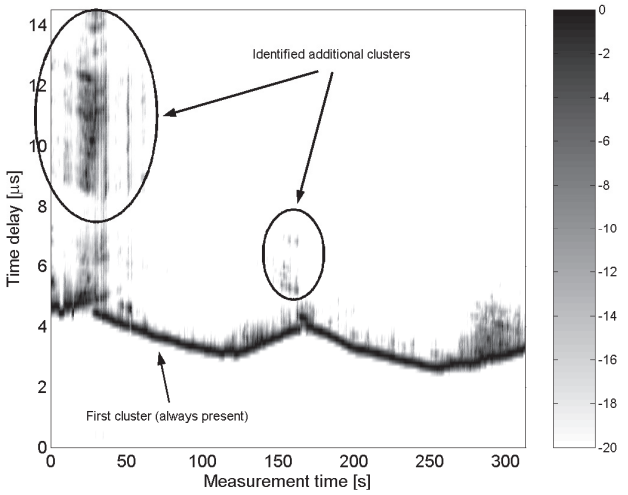

Fig. 1. An example of cluster identification for a set of consecutive power delay profile measurements performed in an urban area. Only delay bins with powers greater than -20 dB relative to that of the strongest delay bin are shown.

as:

$$\underline{h}\left(\overrightarrow{r},\tau,\Omega,\Psi\right)=\sum_{l=1}^{L\left(\overrightarrow{r}\right)}\underline{a}_l\delta\left(\tau-\tau_l\right)\delta\left(\varphi-\varphi_l\right)\delta\left(\theta-\theta_l\right)\delta\left(\varphi'-\varphi'_l\right)\delta\left(\theta'-\theta'_l\right), \quad (1)$$

where (θ,φ) are the elevation and azimuth angles of incidence at the BS, the angles (θ',φ') are the elevation and azimuth angles of departure at the MS, τ is the delay, and $\underline{a}_l$ is a complex polarimetric 2×2 matrix. The description in (1) is intended here to account for only the medium between transmitting and receiving antenna, without the antennas or the transmitter and receiver pulse-shaping filters.

Each of the parameters in (1) varies in space[4] according to specific probability density and autocorrelation functions. These functions (characterized by global parameters) are in turn dependent on the external parameters and the selected radio environment. The following section describes the models and values for the global parameters and how the parameters of the MPCs are generated.

IV. Parameter Models and Settings

The description of global parameters and their models is divided into separate discussions of the channel impulse response, clusters within said impulse response, and finally the MPCs making up a cluster. Most of the global parameters are previously well known channel characterization parameters such as the rms delay spread of a channel, or the Ricean K-factor for characterizing envelope fading. These parameters have been estimated separately in different previous measurement campaigns, which is useful since they can be re-used and combined with similar results from new work. When available the findings of previously published studies of these physical parameters are taken into account.

[4]Time variations are introduced by movement of the MS, $\overrightarrow{r}=\overrightarrow{r}\left(t\right)$, but variations caused by motion in the operating environment, other than the motion of the MS, are not accounted for.

TABLE II
Experimentally Observed Number of Clusters

Environment	Fraction of total meas. time with			Average # of clusters N_C
	1 cluster	2 clusters	3 clusters	
Bad Urban	0.27	0.28	0.45	2.18
Typical Urban	0.87	0.09	0.04	1.17
Suburban Area	0.92	0.08	0.00	1.08
Rural Area	0.94	0.06	0.00	1.06

A. The Number of Clusters

Clustering of MPCs is known to occur on mobile radio channels and has been included in some models [15]-[18]. However, the definition of what actually comprises a cluster varies and makes a comparison of different models difficult. In the analysis below, a cluster is defined as a group of MPCs that have similar delay and that share the same long-term evolution in delay, such that the group remains intact. This is a more simplified definition than outlined in the introduction as the angular domain is not considered. However, visual inspection of a number of measured power-delay-azimuth profiles by the authors showed that both definitions gave the same results in terms of the number of visible clusters. To improve the understanding of how common the clustering effect is, a study of measured data was performed. The data were measured using the TSUNAMI II testbed [60] in the cities of Aarhus, Denmark and Stockholm, Sweden, and in the Danish countryside. Through visual inspection by the authors of series of power delay profiles recorded with 5 MHz bandwidth along measurement routes totaling 32 km in length, the number of clusters present was determined (Table II). The power delay profiles were formed by averaging the squared magnitude of impulse response estimates over a distance of 5-10 m. Only clusters with a peak power within 20 dB of the largest peak in each power delay profile were considered. The value 20 dB was chosen to reflect an upper limit on the signal to interference and noise ratio (SINR) that a wireless multi-user system is typically dimensioned for. In other words, it is considered unnecessary and inefficient to model MPCs that are down by more than 20 dB, since these would be weaker than the power of the noise and interference. An example of cluster identification is shown in Fig. 1.

As can be seen in Table II, the occurrence of more than one cluster is quite uncommon except in the Bad Urban area. Further, it was found that the number of clusters varies slowly but that transitions can be quite sharp, for instance when passing a street corner. Unfortunately there were no measurements available that could be used to characterize the amount of clustering in Hilly Terrain areas. In the modeling outlined below it is therefore assumed that the number of clusters in the Hilly Terrain environment is identical to that in the Bad Urban area. This assumption is based on the fact that there is some degree of similarity in propagation conditions where there are distant hills in the former environment and where there are distant concentrations of high-rise buildings in the latter. However, actual measurement data would certainly be preferable for parameterizing the model if such are made available.

Experience from the above-described study led to the formulation of a dynamic model for the occurrence of clusters. This model is based on geometrical considerations, where the position of a MS determines the number of active clusters. In this model, there always exists at least one cluster that corresponds to local wave interactions at the MS. The occurrence of additional clusters is determined by a number of visibility areas, circular areas with radius R_C, that are generated within the region of operation (see Fig. 2). The generation of visibility areas is discussed in the next section. Each time a MS enters into a visibility area, a corresponding cluster of MPCs is made active (the corresponding group of IOs becomes "visible"), and when the mobile leaves the visibility area the cluster will be deactivated again. A smooth transition from non-active to active is achieved by scaling the relative power of the cluster by a factor A_m^2. The transition function that is used is given, along with an explanation of the physical basis for it, in [2], as

$$A_m\left(\overline{r}_{MS}\right) = \frac{1}{2} - \frac{1}{\pi}\arctan\left(\frac{2\sqrt{2}y}{\sqrt{\lambda x}}\right), \tag{2}$$

with

$$y = L_C + \left|\overline{r}_{MS} - \overline{r}_m\right| - R_C, \tag{3}$$

and

$$x = L_C, \tag{4}$$

where $\overline{r}_m$ represents the center of the circular visibility area, and λ is the wavelength. This transition function is an approximation of the Fresnel integral that describes the field strength at a certain distance behind a perfectly conducting knife-edge. As such, it is well suited to model the smooth but rapid increase of the power in a cluster that can be observed, for instance, when passing a street corner and coming into line-of-sight of the group of IOs that generates the cluster. Even when the energy in the cluster does not come from a limited angular interval, the transition function may still be applicable, but only if the shadowing occurs on a radio path that is common to all MPCs in the cluster.

The first cluster is always active, i.e. $A_1 = 1$. Expressions (3) and (4) result in $A_m = 1/2$ when the mobile has traversed a distance L_C into the visibility area (see Fig. 3), while A_m becomes smaller closer to the edge of the visibility area. The visibility area can thus be considered as having an effective radius (radius of the area where $A_m \geq 1/2$) of approximately $R_C - L_C$. In order to give a constant expectation for the number of clusters that is equal to the associated value of N_C in Table II, the area density of the visibility areas must be

$$\rho_C = \frac{N_C - 1}{\pi\left(R_C - L_C\right)^2}\left[m^{-2}\right] \tag{5}$$

The parameter L_C can be interpreted as the width of the transition region. Reasonable values for R_C and L_C might be on the order of the size of a city block and the width of a city street respectively. In rural areas variations in clustering is expected to be less frequent due to the scarcity of buildings. The suggested values for the macrocell radio environments that are given in Table III are based on these assumptions.

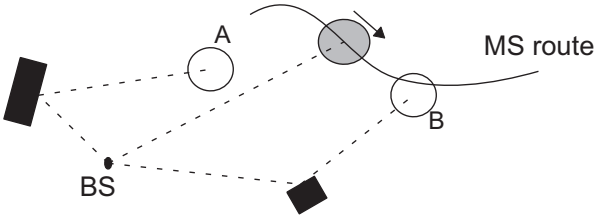

Fig. 2. Example of visibility areas (white circles) and IO positions (black rectangles). The shaded circle is the local scattering cluster, which moves with the mobile station (MS). Along the particular MS route shown, only one of the two clusters (B) will be activated.

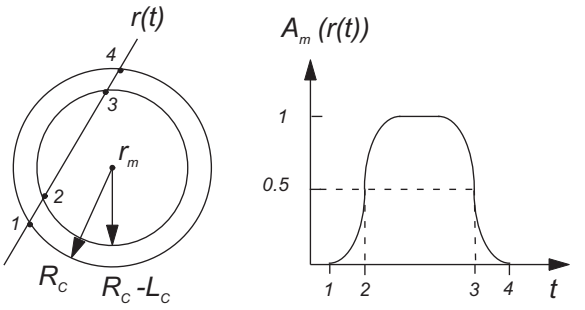

Fig. 3. Activation of cluster using a visibility area and the transition function (1).

B. Cluster Positions

Each cluster is further described by its average azimuth and elevation (as seen from the BS) within a directional channel impulse response estimate and the delay of the first component in the cluster. There are no specific distributions reported in the literature, but there are several examples where cluster directions and delays are found to correspond very well with the directions and distances to high buildings or mountains [31]-[33]. Such IOs can be quite far away from the MS, although the MPC generated by a particular IO becomes weaker as the distance of the IO from the BS and the MS becomes greater. Thus it can be expected that an IO or group of IOs that gives rise to a significant cluster is more likely to be found close to the MS than far from it.

In the model, an IO location, $\overline{r}_{C,m}$, is associated with each cluster. The location is arbitrarily drawn from a two-dimensional Gaussian distribution centered on the corresponding visibility area center, $\overline{r}_m$. The standard deviation of the distribution is equal to $|\overline{r}_m|$.

The delay and azimuth (at the BS) of the cluster occurring due to reception of energy from a particular group of IOs is then given by applying a single-interaction geometrical construction (Fig. 2) which gives:

$$\varphi_m = \begin{cases} \arg\left(\overline{r}_{MS} - \overline{r}_{BS}\right) & m = 1 \\ \arg\left(\overline{r}_{C,m} - \overline{r}_{BS}\right) & m > 1 \end{cases} \tag{6}$$

$$\tau_m = \begin{cases} \frac{1}{c}\left|\overline{r}_{MS} - \overline{r}_{BS}\right| & m = 1 \\ \frac{1}{c}\left(\left|\overline{r}_{MS} - \overline{r}_{C,m}\right| + \left|\overline{r}_{C,m} - \overline{r}_{BS}\right|\right) & m > 1 \end{cases} \tag{7}$$

Motion of the MS, as reflected in changes in $\overline{r}_{MS}$ causes changes in the delay but not azimuth of the clusters. The exception is the first cluster, corresponding to local wave

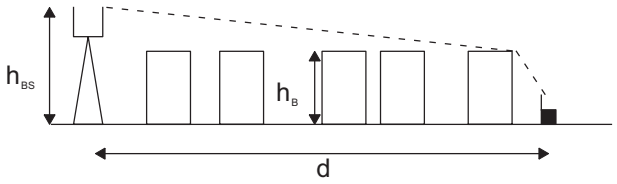

Fig. 4. Elevation angle model.

TABLE III
SUGGESTED VALUES FOR PARAMETERS IN THE CLUSTERING MODEL

	GTU / GBU	GRA / GHT
R_C [m]	100	300
L_C [m]	20	20

interactions only, the azimuth and delay of which will move with the MS.

For simplicity, the elevation angles to distant IOs are assumed to be zero. For the local cluster $(m = 1)$ the elevation angle is calculated assuming a model as in Fig. 4. This model assumes that most of the energy reaches the MS via diffraction over the intermediate buildings, an assumption that has proved useful in modeling path loss [21]-[23]. The average building height h_B, which is an external parameter, is used to determine the elevation in non-LOS conditions. In LOS conditions the MS antenna height h_{MS} is used instead of h_B.

$$\theta_m = \begin{cases} \arctan\left(\frac{h_B - h_{BS}}{d}\right) & m = 1 \\ 0 & m > 1 \end{cases} \tag{8}$$

C. Cluster Path Gains

On a channel having an equivalent impulse response with multiple clusters, the time variations in amplitude of which are uncorrelated, the total path gain[5] P is composed of the sum of the cluster path gains:

$$P = \sum_{m=1}^{M} P_m \tag{9}$$

The assumption of uncorrelated clusters is discussed further in [2].

The path loss incurred on radio channels has been a topic of major interest during the evolution of mobile radio communications, and there are many results and models available. In the following, line-of-sight and the non-line-of-sight cases will be first considered separately. Then, a cluster path gain model that combines the two will be formulated.

1) Line-of-sight: Path loss under line-of-sight conditions can be modeled as either being that which occurs in free space, or using a two-ray (plane earth) model that includes consideration of a ground reflection, depending on distance from the transmitter, and clearance from the ground. The authors have found from various path loss measurements that the ground reflection often does not play a significant role in the macrocellular case. An example of this is the measurements reported in [57], where free space levels of path loss were measured at distances up to 10 km in rural areas.

The area of satellite communication research provides interesting results [24] on the probability of LOS between a land mobile receiver and a satellite. Such results showing a primary dependence upon the elevation angle of a satellite. In a land mobile system there should be a similar dependence, but the distance between BS and MS should also play a part. To confirm this, a study was performed by the authors using a digital building database for the city of Stockholm, Sweden. Site positions were defined on top of some building roofs, with the height of the antenna h_{BS} being a variable. User positions were generated in a uniform grid with 5m resolution, discarding grid points inside buildings. For each distance interval of 50m from a site and each BS height, the fraction of user positions with unobstructed line-of-sight to the site was determined. This simulated probability of line-of-sight was plotted against distance d and the BS antenna height h_{BS}, and an empirical expression was then fit to the results, giving the model:

$$p_{LOS}(d) = \max\left(\frac{h_{BS} - h_B}{h_{BS}} \frac{d_{CO} - d}{d_{CO}}, 0\right) \tag{10}$$

Here h_B is the average building height and d_{CO} is a cut-off distance. The probability decreases with reduced BS antenna height and increased distance, just as expected. Beyond the cut-off distance d_{CO} the probability is zero. A value of $d_{CO} = 500m$ was found appropriate for Stockholm.

2) Non-line-of-sight: Empirical models such as Hata's [20] or approximate solutions like Walfisch-Bertoni [21] can and have been used successfully to predict path loss under non-line-of-sight conditions, especially in conjunction with various extensions [22], [23]. In the COST 231-Walfisch-Ikegami model [22] provisions are made for path loss prediction under both line-of-sight and non-line-of sight conditions.

For clusters other than the first, the cluster path gain P_m is expected to be conditioned on the excess delay $\tau_m - \tau_1$, where τ_1 is the delay of the first cluster, since the extra path length and extra wave interactions would give rise to an added attenuation. An often-used model for indoor propagation is the model by Saleh and Valenzuela [18] with exponentially decaying cluster path gain with respect to excess delay. The trend of decreasing cluster gain with increasing delay is also regularly observed in macrocells, even though the mechanisms that generate clusters are different than in indoor propagation, where isolated IOs are rare.

Path loss models such as those described above give the expectation of P at a given distance. Since the number of clusters and their path gains vary, the expectation needs to be taken over all outcomes of the cluster occurrence process. A practical approach [61] to model the cluster path gains is to determine a distance-dependent correction factor $s(d)$ that relates the expectation of P to the expectation of the total path gain. The path gain of the first and always present cluster, P_1, is then simply modeled by the total path gain divided by $s(d)$, while additional clusters have their path gains modeled by P_1 multiplied with a function that decreases in value with increasing excess delay.

[5]The path gain is the inverse of the path loss.

TABLE IV
SUGGESTED VALUES FOR PARAMETERS IN THE CLUSTER PATH GAIN MODEL

		GTU / GBU	GRA / GHT
NLOS path gain	P_{NLOS}	From COST 231-Walfisch-Ikegami [22]	From COST 231-Hata "Suburban" [22]
Correction factor (determined numerically)	$s(d)$	GTU: $1.36 \cdot d^{-0.03}$ GBU: $5.1 \cdot d^{-0.15}$	GRA: $1.07 \cdot d^{-0.004}$ GHT: $5.1 \cdot d^{-0.15}$
Cluster power	k_τ [dB/μs]	1	1
	τ_B [μs]	10	10
LOS occurrence	d_{co} [m]	500	5000
	R_L [m]	30	100
	L_L [m]	20	20

3) Cluster Path Gain Model: Taking all the above information into account, a cluster path gain model was developed and tuned through comparison of resulting rms delay and angular spreads with those estimated from measured data. The model is formulated as:

$$P_m = \begin{cases} S_1 \frac{P_{NLOS}}{s(d)} + A_L^2 \left(\frac{\lambda}{4\pi d}\right)^2 & m = 1 \\ A_m^2 S_m \frac{P_{NLOS}}{s(d)} 10^{\frac{-k_\tau \min(\tau_m - \tau_1, \tau_B)}{10}} & m > 1 \end{cases} \quad (11)$$

where P_{NLOS} represents the non-LOS path gain, A_L is a transition function for activating the LOS component, S_m is the shadow fading gain which is discussed in more detail in Section IV-E, and A_m is the transition function, given by (2), for activating/deactivating a cluster. The parameters k_τ and τ_B characterize the path gain conditioned on excess delay $\tau_m - \tau_1$ as shown in Fig. 5. An exponential decay is applied up to excess delay τ_B. Beyond this delay the path gain is constant so as to result in the existence of some clusters with significant power at long delays.[6]

The non-line-of-sight path gain P_{NLOS} is obtained using the COST 231-Walfisch-Ikegami model [22] for the urban environments GTU and GBU while the COST 231-Hata model [22] is used for the rural environments GRA and GHT. The correction factor for Suburban Areas should be used in the COST 231-Hata model.

The line-of-sight path gain is modeled by free space path gain multiplied by a transition function A_L^2. The transition function takes on values between zero and one and is used for modeling transitions between line-of-sight and non-line-of-sight. To determine where there is line-of-sight, a dynamic geometrical model with "visibility areas" very similar to the one discussed in Section IV-A is proposed. To comply with the distance-dependent probability of line-of-sight (10), circular areas with radius R_L are distributed with an area density ρ_L.

$$\rho_L(d) = \frac{p_{LOS}(d)}{\pi (R_L - L_L)^2} \left[m^{-2}\right] \quad (12)$$

When a mobile enters one of these circles the transition function A_L is calculated according to (2) but with:

$$y = L_L + |\overline{r}_{MS} - \overline{r}_L| - R_L \quad (13)$$

$$x = L_L \quad (14)$$

[6]Separate modeling of the path loss from the BS to the IOs, the associated interaction loss, and finally the path loss from an IO to the MS was considered during the model development, but the lack of measurements where each of the three was characterized separately prevented this more physically based approach from being pursued.

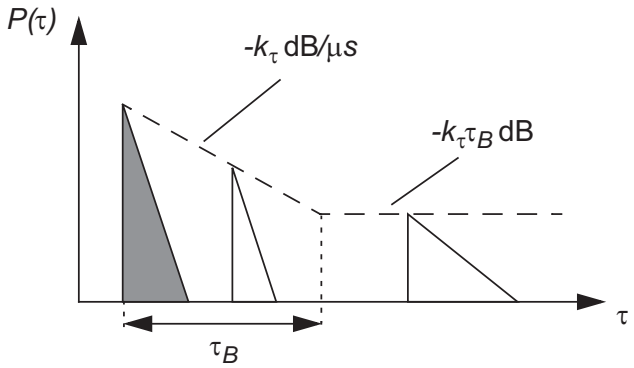

Fig. 5. Cluster power conditioned on excess delay.

In the case of overlapping visibility areas the one giving the highest value of A_L is used.[7]

When selecting appropriate parameter values it is important to consider the influence of *cluster* path gains and *cluster* positions in delay and angle on the *channel* time- and angular dispersion. The suggested parameter values for the cluster path gain modeling listed in Table IV are partly a result of this. Section IV-E will elaborate on this, and a validation that the resulting channel spreads conform to measurements will be performed in Section VI.

In addition to the average path loss discussed in the foregoing, a radio channel is often influenced by slowly varying power fluctuations that can either be a slower form of fading that results from multipath interference at specific ranges from the transmitter, or the result of the spatially varying obstruction of any of several radio paths (including, but not necessarily, the direct one) between the transmitter and receiver by buildings and terrain height variations. This fluctuation is usually referred to as shadow fading or slow fading. Since the paths in different clusters arrive at the MS from different directions, it can be surmised that some clusters may be obstructed while others are not. A separate shadow fading process could then be applied to each cluster. This is in analogy to the shadow fading that occurs on radio paths between one MS and two different BSs [26], where the correlation over the two links is usually low unless both BSs are in the same direction, as seen from the MS. Cluster shadow fading S_m is studied in more detail in Section IV-E.

[7]A renormalization of (11) would be necessary since this expression is derived assuming no overlap. The renormalization could be done analytically or numerically.

D. Cluster Power Delay-Direction Profile

The Power Delay-Direction Profile (PDDP), defined in [2], Eq. (9), for a cluster reflects the average relative power as a function of relative delay and directions within a cluster, and is characterized by the PDDP function $P(\tau, \theta, \varphi, \theta', \varphi')$. Based on the analysis of joint delay-azimuth measurements at a location typical of macrocell base stations, Pedersen et al. [34] reported that the Power-Azimuth-Delay Profile $P(\tau, \varphi)$ could be decomposed into two other functions $P_\tau(\tau) P_\varphi(\varphi)$ in a one-cluster (typical urban) scenario. This decomposition of the PDDP of the *channel* is not possible in a two-cluster (bad urban) scenario, however it is evident from Fig. 14 in [34] that each of the *clusters* can still be decomposed this way. For the elevation domain there are fewer data available, although, it is conjectured here that the results of [31] might support a similar decomposition for $P_\theta(\theta)$. Measurements by Kuchar et al. [56] show how the power-azimuth- and power-elevation-profiles at a MS depend on cluster delay. No studies that show the connection, in terms of joint distributions, between directions at the BS and the MS are available. Until better information becomes available from measurements, it is therefore proposed that the PDDP for each cluster should be represented as:

$$P(\tau, \theta, \varphi, \theta', \varphi') = P_\tau(\tau) P_\theta(\theta) P_\varphi(\varphi) P_{\theta'}(\theta', \tau) P_{\varphi'}(\varphi', \tau). \quad (15)$$

In order for the profile of a cluster to be decomposable in this manner, there would have to be multiple interactions involved since the PDDP of a single-interaction geometric model must exhibit dependencies among the angles at the base and the mobile stations. Furthermore, a receiving antenna would, according to (15), experience the same angular and delay profiles for any cluster, regardless of whether the transmitting antenna illuminates all or just a few of the associated IOs. This can only occur if these IOs in turn illuminate all other IOs with equal intensity.

A benefit of the decomposition in (15) is that information is separately available in the literature for each of the profiles on the right-hand side of the equation. The power-delay profile $P_\tau(\tau)$ has attracted the most attention due to its strong impact on inter-symbol interference, which results in a requirement for equalizers and multipath mitigation. An exponentially decaying power-delay profile (16) seems to be accepted by many [15], [18], [19] as a good model. The exponential profile is characterized by the decay constant σ_τ, which is the well known rms delay spread.[8]

$$P_\tau(\tau) = \frac{1}{\sigma_\tau} e^{-(\tau-\tau_m)/\sigma_\tau} \quad \text{for } \tau \geq \tau_m, \quad 0 \text{ otherwise} \quad (16)$$

The azimuth spread at the base station was first studied indirectly using space diversity measurements [35] where a Gaussian profile was assumed. Later Pedersen et al. [36] showed from direct measurements that a Laplacian function (17) was a better fit than the Gaussian. The parameter σ_φ that characterizes this function is referred to as the azimuth spread.

$$P_\varphi(\varphi) = \frac{1}{\sigma_\varphi \sqrt{2}} e^{-\sqrt{2}|\varphi-\varphi_m|/\sigma_\varphi} \quad (17)$$

[8]Throughout this paper, rms delay spread is to be understood as an expectation over a local area of the second central moment of the squared magnitude of the impulse response.

Description of the elevation characteristics of angles of arrival at a BS present greater problems due to the lack of reported measurements. However, the measurements in [31] indicate that the Laplacian function (18) *could* be a good candidate, and therefore it was selected for the model of the elevation spectrum. The describing parameter in this case is the elevation spread σ_θ.

$$P_\theta(\theta) = \frac{1}{\sigma_\theta \sqrt{2}} e^{-\sqrt{2}|\theta-\theta_m|/\sigma_\varphi} \quad (18)$$

The azimuth and elevation spread at the BS and the delay spread will be discussed further in the next section.

Angular profiles at the MS have mostly been studied indirectly by evaluating the statistics and autocorrelation of the fast fading resulting from motion of the MS. The usual assumption is a uniform power-azimuth profile, which, if there are more than 8-10 components, leads to Rayleigh fading with a Doppler spectrum as reported by Clarke [30]. Rayleigh fading has been reported to be exhibited by the envelope of a channel impulse response estimate in each delay and angle resolution interval at the BS, when measured with a wideband directional channel sounder [44]. Similar results for the delay domain only are presented in [45], although it is found that the envelope in the first resolution interval often has Ricean fading statistics due to LOS or quasi-LOS conditions. Direct measurements of the power-azimuth profile at a MS in urban areas have been reported in [54], while [55] and [56] report on joint delay-angle characteristics. In [55], [56] it is shown that the uniform power-azimuth profile as found in [54] among others is valid for small excess delays, while waves with larger delays typically impinge from the directions of the street canyon. Gaussian [54] or uniform [14] distributions have been proposed to model the measured power-elevation profiles. Elevation angles have been found to have a large spread at low delays that decreases as cluster delay increases [56].

Incorporating these findings results in a more complex structure than that required for the profiles in (16)-(18), since the shape is modeled differently for the first cluster compared with additional clusters. For the first cluster $(m = 1)$, a uniform azimuth distribution is used in the COST 259 model for waves with delay less than τ_C, and a combination of two Laplacian distributions is used when the cluster delay is beyond τ_C, which is shown at the top of the next page.

Here $\sigma_{\varphi'}$ is the azimuth spread and φ'_A and φ'_B are the directions of the street canyon in which the MS is located. These directions can be obtained directly from road orientation φ_R, i.e. by $\varphi'_A = \varphi_1 - \varphi_R$ and $\varphi'_B = \varphi_1 - \varphi_R + \pi$. Delayed clusters are characterized by a single Laplacian distribution around the direction φ'_m of the associated IO:

$$P_{\varphi'}(\varphi', \tau) = \frac{1}{\sigma_{\varphi'} \sqrt{2}} e^{-\sqrt{2}|\varphi'-\varphi'_m|/\sigma_{\varphi'}}. \quad (20)$$

Elevation angles are modeled using a uniform distribution between 0 and a delay-dependent maximum angle:

$$P_{\theta'}(\theta', \tau) = \frac{1}{\theta'_{\max}(\tau)} \quad 0 \leq \theta' \leq \theta'_{\max}(\tau). \quad (21)$$

For rural environments (GRA,GHT) the maximum elevation angle $\theta'_{\max}$ is a constant. However, for urban environments

$$P_{\varphi'}(\varphi',\tau)=\begin{cases}\frac{1}{2\pi} & \tau<\tau_1+\tau_C\\ \frac{1}{\sigma_{\varphi'}2\sqrt{2}}\left(e^{-\frac{\sqrt{2}|\varphi'-\varphi'_A|}{\sigma_{\varphi'}}}+e^{-\frac{\sqrt{2}|\varphi'-\varphi_B|}{\sigma_{\varphi'}}}\right) & \tau\geq\tau_1+\tau_C\end{cases} \tag{19}$$

TABLE V
PARAMETERS FOR THE MOBILE DOA MODEL

	GTU / GBU	GRA / GHT
$\sigma_{\varphi'}[^\circ]$	10	10
$\tau_C[\mu s]$	0.4	∞
$\theta'_{max}[^\circ]$	From eq. (22)	15
$\tau_{\theta'}[\mu s]$	3	3

TABLE VI
MEDIAN AZIMUTH SPREADS TAKEN FROM REPORTED MEASUREMENTS IN THE LITERATURE

Reference	Environment	Median azimuth spread [°]
Pedersen et al. [38]	Urban	5-10
Pajusco [39]	Urban	17
	Rural	2.5
Nilsson et al. [40]	Urban	8
	Suburban	5
Pettersen et al. [41]	Urban	7-12
	Suburban	13-18

(GTU,GBU) it is a function of the delay τ, average building height h_B, street width w and the parameter $\tau_{\theta'}$ which determines the rate of its decrease with delay:

$$\theta'_{\max}(\tau)=\frac{1}{1+(\tau-\tau_1)/\tau_{\theta'}}\arctan\left(\frac{2h_B}{w}\right). \tag{22}$$

Parameter values for the cluster power-azimuth- and power-elevation-profiles at the MS are given in Table V. The values were selected to conform with the results in [56].

The cluster shapes proposed in (19)-(21) will result in Rayleigh statistics for fast fading of the cluster envelope. To realize Ricean-fading statistics, as found in [45], the cluster shape function (15) must be modified by adding a single, coherent, MPC to the first cluster, giving Eq. (23), where K_0 is the ratio between the power in the coherent MPC and the diffuse components of the cluster. This parameter is discussed in Section IV-F.

E. Cluster Spreads and Shadow Fading

Unfortunately, results reported in the literature are almost exclusively for *channel* parameters and not for *cluster* parameters. Since the COST 259 model is characterized by cluster parameters the difference between channel parameters and cluster parameters needs to be considered. For instance, the channel rms delay spread is a function of the cluster delay spreads, but also of the cluster powers and positions in delay. The only time it is certain that the cluster parameters and the channel parameters coincide is when there is only one cluster in the channel. However, from Table II it is known that this is commonly the case except in Bad Urban or Hilly Terrain environments. When multiple clusters do occur the channel spreads can be expected to increase by a significant amount compared to the situation when there is only a single cluster. As shall be reported in the following, a channel's rms delay spread and its rms angular spread in azimuth and elevation at the BS can be modeled as mutually correlated lognormal stochastic parameters. Since the lognormal distribution has a rather extended tail, it is considered reasonable, therefore, to assume that the tail is caused by the relatively rare instances in which there are multiple clusters. This allows the cluster spread to be modeled by the same distribution but with a lower spread. For the cluster shadow fading gain a similar argument can be applied.

A very thorough review of rms delay spread measurements is given by Greenstein et al. [29] who also proposes a model to capture the trends found in the data. The model takes into account the lognormality and distance dependence of the rms delay spread, and the correlation of rms delay spread with shadow fading. An extension of this model that also considers the angular spreads forms part of the COST 259 DCM, as will be described below.

There seems to be many similarities between BS angular spreads and delay spreads on macrocellular channels. A visual inspection of various azimuth spread measurements [38]-[40], [58] shows that a lognormal distribution might indeed be a good approximation here also. Azimuth spread is shown to be correlated with shadow fading in [42], [58]. A correlation between the delay spread and the azimuth spread of the channel has also been found [34], [40], [43], [58]. Chu [37] finds a weak trend of decreasing azimuth spread with distance from indirect analysis through measured diversity cross correlations, and Martin [33] finds a decreasing trend with distance in direct measurements of the azimuth spread. Pedersen [38] shows examples of increasing, constant, and even decreasing azimuth spread. Table VI gives a summary of published results on azimuth spreads. In the COST 259 DCM, the angular spread at a BS is modeled by a lognormal distribution having correlation with both rms delay spreads and shadow fading. No distance-dependence is assumed, due to the partly conflicting reports from the literature.

Only one direct measurement of the elevation spread at a BS has been found [31]. However several references [35], [46]-[49] report on envelope cross-correlation statistics for vertically separated antennas. Assuming a Laplacian elevation spectrum, the elevation spread can be calculated from measured CW envelope fading cross-correlations using [38], Eq. (12). The results are summarized in Table VII. As can be seen, the estimated elevation spreads are mostly on the order of one degree or less. After consideration of the above-described information, it has been decided most expedient that the COST 259 DCM should model BS elevation spreads using

$$P_1(\tau,\theta,\varphi,\theta',\varphi') = \frac{1}{1+K_0}P_\tau(\tau)\,P_\theta(\theta)\,P_\varphi(\varphi)\,P_{\theta'}(\theta',\tau)\,P_{\varphi'}(\varphi',\tau) + \frac{K_0}{1+K_0}\delta(\tau-\tau_1)\,\delta(\theta-\theta_1)\,\delta(\varphi-\varphi_1)\,\delta(\theta'+\theta_1)\,\delta(\varphi'+\varphi_1) \quad (23)$$

TABLE VII
ELEVATION SPREADS DERIVED FROM PUBLISHED VERTICAL DIVERSITY MEASUREMENTS

Reference	Typical distances [m]	Vertical separation [λ]	Envelope correlation	Estimated elevation spread [°]
Adachi et al. [35]	1300	12	0.7	0.70
Eggers et al. [46]	500-3000	12.3	0.64	0.79
Ebine et al. [47]	1000-4000	16	0.42-0.65	0.59-0.95
Lundgren and Robertsson [48]	1200-7400	22-50	0.7	0.17-0.38
Turkmani et al. [49]	250-1500	15	0.12-0.56	0.7-2.3

TABLE VIII
SHADOWING PARAMETERS IN THE LITERATURE

Reference	Standard deviation [dB]	Autocorrelation distance [m]
Mockford et al. [25]	4.5	~ 100
Mawira [26]	4	100
	3	1200
Gudmundson [27]	7.5	500
Sørensen [48]	5	5.5

TABLE IX
PARAMETERS FOR THE CLUSTER SPREAD AND SHADOW FADING MODEL

Parameter (source for value)		GTU / GBU	GRA / GHT
Shadow fading (Table VIII)	s_{shf} [dB]	6	6
Azimuth spread (Table VI)	$m_{s\varphi}[^\circ]$	10	5
	$s_{s\varphi}$ [dB]	3	3*
Elevation spread (Table VII)	$m_{s\theta}[^\circ]$	0.5	0.25
	$s_{s\theta}$ [dB]	3*	3*
Delay spread (Greenstein [29])	$m_{s\tau}[\mu s]$	0.4	0.1
	ϵ	0.5	0.5
	$s_{s\tau}$ [dB]	3	3
Autocorrelation distances (Table VIII,[58])	$L_S, L_\tau, L\varphi, L_\theta$ [m]	100(*)	100(*)
Cross-correlations ([29],[58])	ρ_{XY}	-0.75	-0.75*
	ρ_{XZ}	-0.75	-0.75*
	ρ_{YZ}	0.5	0.5*

*Parameter value is not available in any measurement

a lognormal distribution that has no correlation with rms delay spread, azimuth spread or shadow fading.

The accepted model for shadow fading is a lognormal distribution with an exponentially decaying autocorrelation function [27], or a combination of two such processes with different autocorrelation lengths [26]. Some published results are summarized in Table VIII. The variations among the different results can be partly explained by different averaging lengths [25]. Algans [58] also finds the autocorrelation functions for the delay spread and azimuth spread to be well modeled by an exponentially decaying function. Consideration of this information resulted in a decision that the COST 259 DCM should use a single lognormal process to model shadow fading variations, and exponential autocorrelation functions for all the cluster spreads.

The complete model used in the COST 259 DCM for shadow fading of cluster envelopes and angular spreads at the BS is thus a variant of the model by Greenstein [29], and is formulated in terms of the cluster spreads $\sigma_{\tau,m}$, $\sigma_{\varphi,m}$ and the cluster shadow fading gain S_m according to the following:

$$S_m = 10^{s_{shf}X_m/10} \quad (24)$$

$$\sigma_{\varphi,m} = m_{S\varphi}10^{s_{s\varphi}Y_m/10} \quad (25)$$

$$\sigma_{\tau,m} = m_{S\tau}\left(\frac{d}{1000}\right)^{\varepsilon}10^{s_{s\tau}Z_m/10} \quad (26)$$

where X_m, Y_m, Z_m are random Gaussian variables with zero mean, unit variance, and cross-correlations $\rho_{XY}, \rho_{XZ}, \rho_{YZ}$. The correlation between realizations of each of these parameters for different clusters is zero, i.e. $\rho_{X_mX_n} = \rho_{Y_mY_n} = \rho_{Z_mZ_n} = \delta_{mn}$ where δ_{mn} is the Kronecker delta.[9] The

[9]The Kronecker delta is defined as $\begin{cases} \delta_{mn}=1, & m=n \\ \delta_{mn}=0, & m\neq n \end{cases}$

random variables X_m, Y_m, Z_m have exponential autocorrelation functions with autocorrelation lengths $\{L_S, L_\tau, L_\varphi\}$. The parameters $s_{shf}, s_{s\tau}, s_{s\varphi}$ are standard deviations expressed in dB. The median azimuth spread is $m_{s\varphi}$ while $m_{s\tau}$ is the median delay spread at a distance $d = 1000m$ from the associated BS. The dimensionless exponent ε determines the distance dependence of the delay spread, as reported in [29].

The BS elevation spread is modeled as uncorrelated with the other cluster spreads. This model also employs a lognormal distribution:

$$\sigma_{\theta,m} = m_{s\theta} 10^{s_{s\theta} W_m / 10} \tag{27}$$

where W_m is a random Gaussian variable with zero mean, unit variance, and exponential autocorrelation function with autocorrelation length L_θ.

Table IX lists the suggested parameter values for the four radio environments that can be specified when using the model. Values are mainly taken from [29] with a low-end value for $s_{s\tau}$ to account for the cluster spread as opposed to the channel spread. The azimuth spread and elevation spread parameters are based on information in the references cited above, or, when such is lacking, by assuming identical values as for the delay spread.

F. Fading Statistics

The envelopes of narrowband signals received over fading radio channels are well known to often vary with Rayleigh or sometimes Ricean distributions. In a directional wideband channel model the fading statistics in each resolvable delay/angle bin are of interest. The fading in each such bin has been reported to be approximately Rayleigh distributed when measured with a resolution capability of $244\text{ns}\times 5^\circ$ [44]. For a similar bandwidth [45] also reports very small Ricean K-factors (i.e. specular/random power ratios) for all delay bins except the first. There is less conclusive evidence for cases where greater communication bandwidths are assumed, although in some such cases similar behavior has been observed.[10] The COST 259 model therefore imposes Rayleigh fading in all resolvable delay/angle bins but with a strong, persistent MPC added (23) to give Ricean fading in the first bin. Based on the observations of fading behavior reported above, this is considered to be a reasonable approximation for bandwidths up to 50 MHz, although it is acknowledged that there are likely scenarios where the fading behaves differently.

The average power ratio between the added component and all other multipath components in the channel model is characterized by the narrowband/widebeam Rice-factor K_0. An evaluation of narrowband fast fading statistics extracted from the same measurement data as that used to derive parameters discussed in Section IV-A was performed by the authors. The value of K_0 was estimated from the fast fading variations in data recorded on each local segment (a few meters in length) along a measurement route using the moment method reported in [64]. These estimates were further grouped according to the excess path loss in dB, L_E, on the local segment. Each group consisted of a 10 dB excess path loss interval. It was found that the K_0 estimates in each group could be described by a lognormal distribution, i.e. a Gaussian distribution in dB. The standard deviation of this distribution was about 6 dB in each group, but the mean value was clearly dependent on the excess path loss. The empirical expression (28) was obtained from linear regression of this dependence. A global autocorrelation distance of 8 m was found for the variations in K_0, however local variations could be significantly slower or faster than this.

$$m_K = \frac{26 - L_E\,[dB]}{6} \tag{28}$$

This behavior is modeled by letting K_0 be a lognormal parameter with mean m_K according to (28), standard deviation σ_K and an exponential autocorrelation function with correlation length L_K. These parameters are summarized in Table X. The introduction of a strong, persistent MPC in the first cluster of course affects the rms delay spread and angular spread, mainly by increasing the probability for low spreads.

G. Multipath Components

In this section the substructure of a cluster, i.e. its complement of MPCs, is discussed. With the PDDPs, the positions, and the relative powers of the clusters set, all that remains is to simulate the MPCs that make up each cluster. Three choices remain, namely the choice of probability distributions in delay and angle $p_\tau(\tau)$, $p_\varphi(\varphi)$, $p_\theta(\theta)$, $p_{\varphi'}(\varphi')$, $p_{\theta'}(\theta')$, and the choice of power conditioned on delay and angle, $p_P(P|\tau,\theta,\varphi,\theta',\varphi')$, and the number of MPCs that should be considered in the channel model.

There are studies such as [17], [44] that could help in determining which probability distributions should be used. However, the COST 259 DCM relies on modeling the effective MPGs rather than the physical MPCs that would be visible with sufficiently high resolution. This gives a certain freedom in selecting the probability distributions, since any combination of pdf's that result in the power profiles described in (15)-(21) can be used. Perhaps the simplest choice is uniform distribution of MPCs in angle and delay; the power conditioned on angle and delay will then be given directly by the functions (15)-(21). Other choices may be more advantageous for implementation.

The model requires that Rayleigh fading should result in each resolvable delay bin. This means that a certain number of MPCs needs to be present in each such bin to provide a good approximation of Rayleigh fading. The exact number depends on how good the approximation needs to be and may vary from one simulation study to another. However, 10-15 roughly equal powered MPCs per bin is often sufficient. The resolution capabilities of the system to be studied in combination with the cluster spreads determine how many bins each cluster will span, and consequently the total number of MPCs needed to accurately model the channel.

H. Polarization

The polarization of an MPC is modeled by a 2×2 polarimetric matrix [2], Eq. (2). However, there is a dearth of information in the literature regarding the characteristics of this matrix, since published measurements have usually

[10]In a measurement with 200 MHz bandwidth in a macrocell outdoor to indoor scenario the authors have observed very low Rice factors in all but a few delay bins.

TABLE X
PARAMETERS FOR THE FAST-FADING MODEL

	GTU / GBU / GRA / GHT
σ_K [dB]	6
L_K [m]	8

TABLE XI
PARAMETERS FOR THE MPC POLARIZATION MODEL

	GTU / GBU	GRA / GHT
$\begin{bmatrix} \chi_{vv} & \chi_{vh} \\ \chi_{hv} & \chi_{hh} \end{bmatrix}$ [dB]	$\begin{bmatrix} 0 & -6 \\ -6 & 0 \end{bmatrix}$	$\begin{bmatrix} 0 & -12 \\ -12 & 0 \end{bmatrix}$
σ_χ [dB]	3	3
L_χ [m]	8	8

reported the polarization of narrowband signals, rather than distinct MPCs. For narrowband signals, it has been reported that the fast fading of different components of the channel polarization matrix (i.e. orthogonally polarized signals) is not correlated (for a vertical/horizontal polarization split)[11] [50], [51], [52], and that the channel polarization matrix can be characterized by the average relative powers of its components. The ratio between cross-polarized (off-diagonal) and co-polarized (on-diagonal) power is reported to be in the range 4-8 dB in urban environments and 9-15 dB in suburban [40], [46], [49], [50], [51], [53]. Lee [50] reported that H-H and V-V have equal power, a result that is supported by Turkmani [49], while Lotse [51] reported that the H-H component has 6-11 dB lower power than V-V.[12] Lee [50] also found that the power ratio between the local means on different (H and V) polarizations has a lognormal pdf with a standard deviation of 2 dB. Available literature suggests that other channel parameters such as the mean azimuth angle of arrival [44], azimuth spread [44], [40], and rms delay spread [40], [46] are independent of polarization.

In the COST 259 DCM, the complex polarization matrix $\underline{\alpha}_l$ of an MPC [2] is modeled by:

$$\underline{\alpha}_l = \begin{bmatrix} \sqrt{g_{vv}}\exp(i\beta_{vv}) & \sqrt{g_{vh}}\exp(i\beta_{vh}) \\ \sqrt{g_{hv}}\exp(i\beta_{hv}) & \sqrt{g_{hh}}\exp(i\beta_{hh}) \end{bmatrix} \tag{29}$$

where the relative phases for the four possible combinations of transmit and receive polarizations, $\{\beta_{vv}, \beta_{vh}, \beta_{hv}, \beta_{hh}\}$, are independently uniformly distributed between 0 and 2π and the relative powers $\{g_{vv}, g_{vh}, g_{hv}, g_{hh}\}$ are independently lognormally distributed according to $g = 10^{G/10}$ where the Gaussian variable G has a mean χ and a standard deviation σ_χ. Large-scale variations in the polarization matrix are determined by an exponentially decaying autocorrelation function for G with autocorrelation length L_χ. Parameter values for the polarization model were selected based on the above-cited references and are summarized in Table XI.

[11]V and H should be interpreted as E_θ and E_φ, defined in a spherical coordinate system centered on the antenna.

[12]The results by Lotse are based on the assumption that the distribution of incident waves at the mobile are in the horizontal plane.

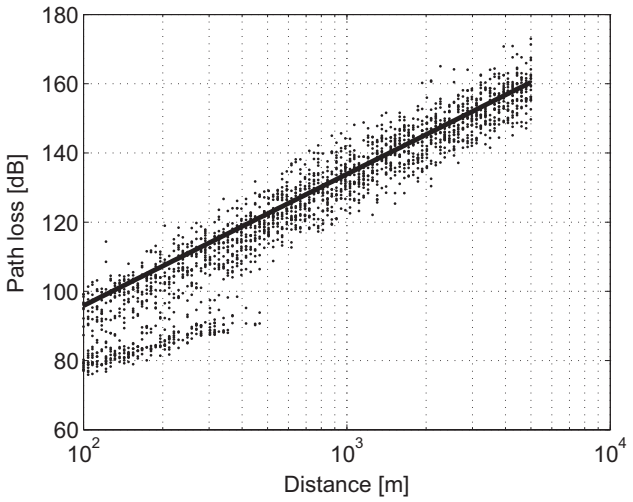

Fig. 6. Comparison of simulated path loss for the GBU radio environment (dots) and the COST 231-Walfisch-Ikegami model (solid line). The standard deviation of the GBU path loss in non-LOS conditions around a linear regression line is 6.0 dB. The influence of LOS conditions, resulting in lower path loss, can be seen at small distances.

V. IMPLEMENTATION

Implementation of the model proposed in this paper is a complex task compared to that of implementing previous models, due to the combined modeling of small-scale and large-scale effects. The model flow outlined in Fig. 2 of [2] can be used as a guide. In this scheme, the local movement of the mobile is compared with the size of the local area, which is defined as the area over which all large-scale parameters can be viewed as constants [2]. The large-scale parameters are updated when the movement exceeds the size of the local area. Since large-scale variations occur at a low rate, the main computational complexity is in generating the local impulse response by superposition of plane waves. This makes the computational effort no different than for more simple channel models.

VI. MODEL VALIDATION

The various sub-models for cluster and MPC behavior have been described in Section IV. To complete the validation, the result of combining these sub-models into a channel model must be analyzed and compared with available measurements. To this end a large number of channel realizations were generated that simulate conditions at various distances of the MS from the BS using an implementation of the proposed model in Matlab. The typical values for the external parameters given in Table I were used, and a carrier frequency of 2 GHz was assumed. The simulation results were then analyzed using the same methods as those used for the analysis of measured data. All of the analyses were performed on the same realizations to ensure that the model simultaneously compared favorably with the available measurement data on different channel characteristics. Comparisons are presented below.

A. Path Loss and Shadow Fading

A local average of the channel path loss was obtained by averaging 100 realizations within a local area of 20λ

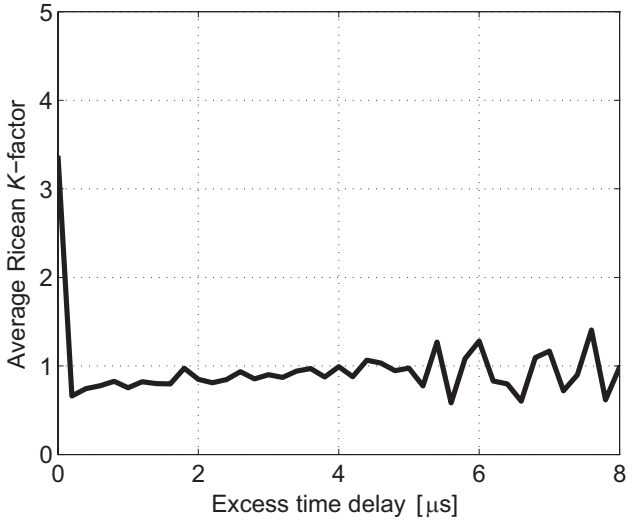

Fig. 7. Global average fading delay profile for a uniform distribution of users in a GTU radio environment.

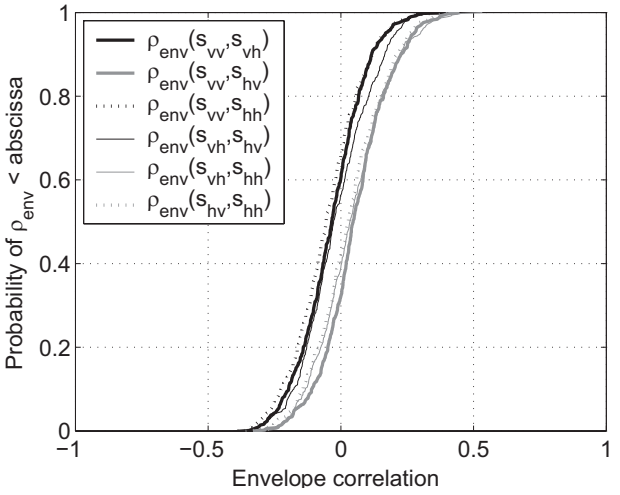

Fig. 8. Envelope cross-correlation between fast fading of signals with different combinations of polarization at the BS (first sub-index) and the MS (second sub-index) in a GTU radio environment.

(3m). Fig. 6 compares the path loss for the cluster-rich GBU radio environment with the COST 231-Walfisch-Ikegami model using the same external parameters. The GBU path loss follows, on average, the COST231-Walfisch-Ikegami model very well, except at distances less than 500 m from the BS, where the occurrences of line-of-sight lead to greater signal powers than those reflected by the COST 231-Walfisch-Ikegami model. Shadow fading in non-line of sight conditions for the simulated channels was found to be well represented by a lognormal distribution with a standard deviation of 6.0 dB, which compares well with the measured values reported in Table VIII. At distances less than 500 m from the BS, the standard deviation is significantly greater as a result of the more frequent occurrence of line-of-sight conditions.

B. Fast Fading

Channel realizations for the GTU radio environment were used to determine fast fading statistics of simulation results for a local area. A moment method [64] was then applied to estimate the Ricean K-factor from the local fading variations in each 200 ns bin in simulated equivalent channel impulse response functions. Fig. 7 shows the global average fading delay profile [45], defined as the global average of the K-factor vs. excess delay. The K-factor is equal to or slightly less than one in all delay bins except the first, where the average K-factor is greater. A K-factor of one is strictly speaking not Rayleigh fading as that would require $K = 0$, and hence the simulated channels appear to deviate from the model assumption of Rayleigh fading. However, the explanation is likely a different one, namely that the K-factor estimator is biased towards higher K-factors for near-Rayleigh fading and finite data samples. When applying the estimator to a simulated zero-mean complex Gaussian process with the same number of independent data samples as used when determining the fading delay profile in Fig. 7, the average estimated K-factor was almost 0.6. The behavior of the simulated channel impulse response functions matches the measured fading delay profiles reported in [45], Fig. 4.

C. Polarization

The complex polarization matrix associated with the model of a narrowband channel was also calculated for a large number of GTU channel realizations. The envelope cross-correlation between fast fading variations on each of the four elements in the polarization matrix, calculated over the 100 local realizations, was invariably low, as can be seen in Fig. 8. Correlation was less than 0.3 for over 90% of the receive locations and among all combinations of elements. Average powers of the cross-polarized components $(V - H, H - V)$ were 6 dB lower than the co-polarized $(V - V, H - H)$, and the two co-polarized components had average powers within 0.1 dB of each other. These results all conform very well to the findings of Lee [50].

D. Azimuth and Elevation Spread

Cumulative distributions of azimuth spreads at the BS, calculated from channel realization in GTU and GBU, are shown in Fig. 9. For comparison, the measured distributions reported in [34] are also shown. The area in Stockholm where the measurements were performed can be characterized as "Bad Urban" due to large areas of open water in the city centre, while Aarhus is a city with fairly uniform building heights that would correspond to a "Typical Urban" environment. The COST 259 model gives a reasonably good representation of the measured azimuth spreads, including an increase in values for the GBU case, as compared to values for the GTU case. Median azimuth spreads are 7.5° for the GTU case, and 12.5° for the GBU case, values that correspond well with the other measurements reported in Table VI.

The BS elevation spread was analyzed by determining the envelope cross-correlation of the simulated fast fading of signals received on vertically separated isotropic BS antennas with different separations. The fast fading was generated through a simulation of motion by the MS antenna within a local area. Fig. 10 shows the mean, 10th, and 90th-percentiles of the envelope correlation at different vertical BS antenna

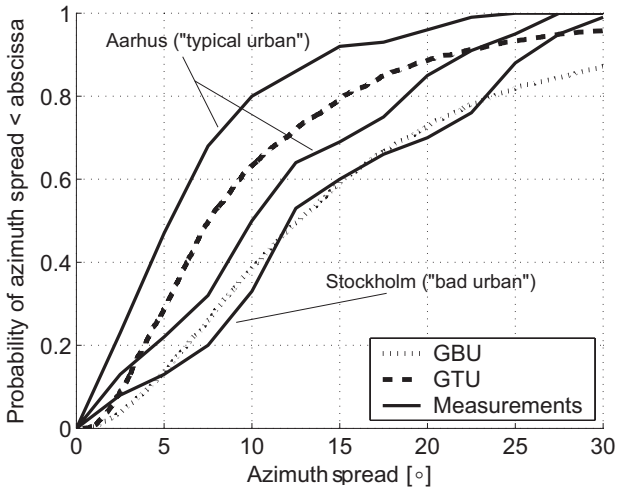

Fig. 9. Cumulative distributions of rms azimuth spread for channel realizations pertinent to GTU and GBU radio environments and from measurements by Pedersen et al. [34].

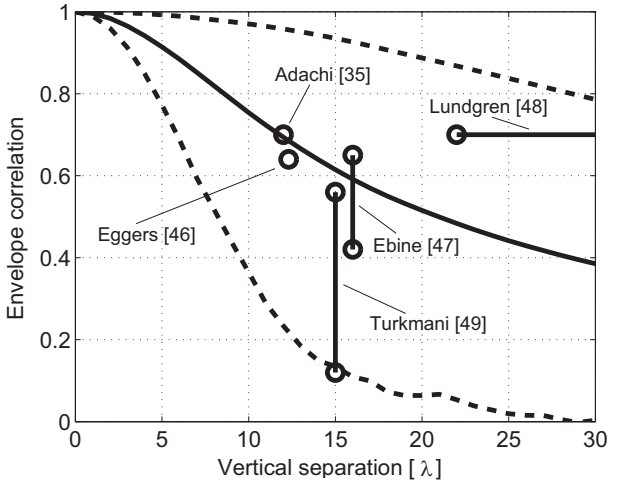

Fig. 10. Mean envelope cross-correlation function (solid) and 10- and 90-percentiles (dashed) of fast fading variations for vertically separated base station antennas for channel realizations from the GTU radio environment. Some measured cross-correlation results have been plotted for comparison.

separations for a large number of channel realizations representing conditions in a GTU radio environment. The measured correlation values that are listed in Table VII have been plotted for comparison, and can be seen to fall in the range spanned by the simulated channels. Since envelope correlation is mainly dependent on the elevation spread[13] this leads to the conclusion that the model and the measurements have similar elevation spreads.

E. RMS Delay Spread

The statistics of the rms delay spread values were analyzed for three distances from the BS, 0.5 km, 1 km and 2 km, and for simulations pertinent to both the GTU and the GBU radio environments. Fig. 11 shows the cumulative distributions of rms delay spreads for simulated results corresponding to

[13]This is true for high correlation values (> 0.7). For lower correlation values the shape of the Power-Elevation spectrum is also important.

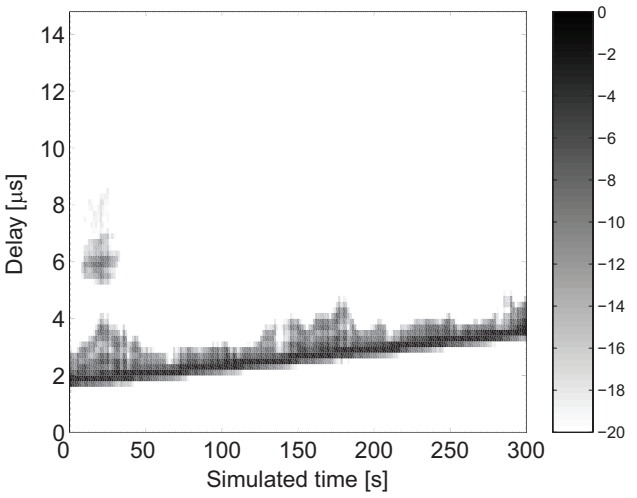

Fig. 12. Dynamic evolution of power delay profiles for a mobile route in a GTU environment. A 5 MHz band-limiting filter was applied to the modeled channel impulse response functions.

the two different environments, together with the lognormal distributions given by the model published by Greenstein et al. [29] and measured distributions from the city of Stockholm, Sweden, found from analysis of the data described in Section IV.A. The minimum and maximum recommended values for the median rms delay spread for urban scenarios, 0.4 μs and 1.0 μs were chosen to reflect "typical" and "bad" conditions for the Greenstein model. The distributions generated by the COST 259 are very similar to those generated by the Greenstein model in the GTU case, including the distance dependence. For the GBU case the correspondence is not as good, both with regard to the shape of the distribution and the distance dependence. This exemplifies the difficulty in selecting cluster parameters that accurately produce certain channel statistics. Nevertheless, the GBU results give a reasonable approximation to the Greenstein model. Both models also compare well with the measurements, considering that these represent a few measurement routes in one particular city, whereas Greenstein's model was compiled from measurements in many different cities.

F. Large-Scale Variations and Clustering

An example of the dynamic evolution of simulated instantaneous power delay profiles for a MS moving in a GTU environment is shown in Fig. 12. The time evolution is visually similar to that of the measured instantaneous power delay profiles in Fig. 1, both with regards to the occurrence and disappearance of an additional cluster, and the dynamics of the delay spread. While the geometry of the routes and the locations of the IOs were most certainly not the same for the measurements and the model, the two figures could, at a glance, be believed to be from the same measurement series. The average number of clusters present in the simulated results was estimated using the same 20 dB peak power threshold as in section IV.A. For a uniform distribution of users within 1500m from the base station, the averages are 1.17 (GTU), 2.28 (GBU), and 1.04 (GRA). These values conform quite well to the values in Table II.

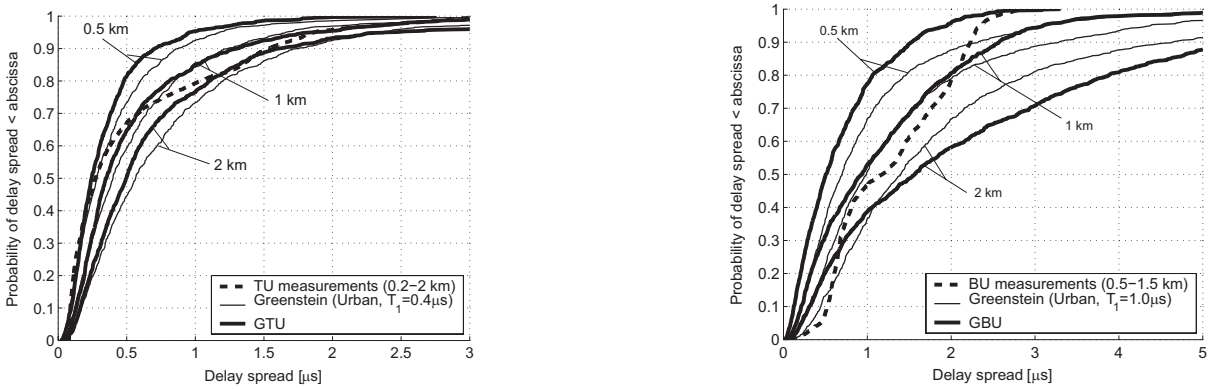

Fig. 11. Cumulative distributions of rms delay spread at three different distances from the base station. A comparison of channel realizations for GTU (left plot) and GBU (right plot) with the delay spread model by Greenstein [29] and with measurements in typical urban and bad urban areas in Stockholm, Sweden. The curves for the Greenstein's lognormal model have been calculated using the medians T_1 of 0.4 μs and 1.0 μs respectively, and with standard deviation $\sigma_y = 4dB$.

VII. Conclusion

The previous section has shown evidence that the COST 259 directional channel model produces simulation results that are simultaneously similar to propagation measurement results for path loss, shadow fading, fast fading of energy within 200 ns bins in impulse response estimates, average relative powers and correlations among co- and cross-polarized components, angular spread and delay spread. However, the measurements do not cover all frequency ranges or radio environments that the model was developed to apply to. In addition, there are few reported data available for some of the channel characteristics, such as the joint behavior of the azimuth and elevation angles of MPCs at a BS and a MS. More work on measuring these channel characteristics is needed as an input to future channel modeling. The COST 259 channel model can be used as a basis for an improved channel model, due to its modular structure that allows exchanges and additions of sub-models or radio environments as more data become available.

While the combined modeling of large-scale and small-scale variations results in realistic channel behavior, it also imposes the burden of increased simulation time to generate a statistically significant sample of channel realizations. A (directional) model with only small-scale variations can be obtained by setting large-scale parameters to deterministic, typical values. Such a model would be suitable for single-link simulations. A small-scale model derived from the COST 259 model has been specified in the standardization of third-generation mobile radio systems [62]. For simulations with multiple simultaneous links, the distribution of users over a large area helps in ensuring that the large-scale channel statistics are sufficiently represented.

References

[1] L. M. Correia, ed., *Wireless Flexible Personalized Communications–COST 259: European Co-operation in Mobile Radio Research*. New York: John Wiley & Sons, 2001.

[2] A. F. Molisch, H. Asplund, R. Heddergott, M. Steinbauer, and T. Zwick, "The COST 259 directional channel model – I. Overview and methodology," *IEEE Trans. Wireless Commun.*, to appear.

[3] A. F. Molisch, J. E. Dietert, R. Heddergott, M. Steinbauer, and T. Zwick, "The COST 259 directional channel model - III. Micro- and picocells," to be submitted.

[4] R. B. Ertel, P. Cardieri, K. W. Sowerby, T. S. Rappaport, and J. H. Reed, "Overview of spatial channel models for antenna array communication systems," *IEEE Pers. Commun.*, vol. 5, no. 1, pp. 10-22, Feb. 1998.

[5] J. C. Liberti and T. S. Rappaport, "A geometrically based model for line-of-sight multipath radio channels," in *Proc. IEEE VTC*, May 1996, pp. 844-848.

[6] P. Petrus, J. H. Reed, and T. S. Rappaport, "Geometrically based statistical model for macrocellular mobile environments," in *Proc. IEEE Globecom*, Nov. 1996, pp. 1197-1201.

[7] M. Lu, T. Lo, and J. Litva, "A physical spatio-temporal model of multipath propagation channels," in *Proc. IEEE VTC*, May 1997, pp. 810-814.

[8] J. Fuhl, A. F. Molisch, and E. Bonek, "A unified channel model for mobile radio systems with smart antennas," in *IEE Proc. Radar, Sonar, and Navigation*, Feb. 1998, vol. 145, no. 1, pp. 32-42.

[9] O. Nørklit and J. Bach Andersen, "Diffuse channel model and experimental results for antenna arrays in mobile environments," *IEEE Trans. Antennas Propagat.*, vol. 46, no. 6, pp. 834-840, June 1998.

[10] P. C. F. Eggers, "Angular dispersive mobile radio environments sensed by highly directive base station antennas," in *Proc. IEEE PIMRC*, Sep. 1995, pp. 522-526.

[11] P. C. F. Eggers, "Angular propagation descriptions relevant for base station adaptive antenna operation," *Kluwer: Wireless Personal Communications*, vol. 11, no. 1, pp. 3-29, Oct. 1999.

[12] U. Martin, J. Fuhl, I. Gaspard, M. Haardt, A. Kuchar, C. Math, A. F. Molisch, and R. Thomä, "Model scenarios for directional-selective adaptive antennas in cellular mobile communication systems-Scanning the literature," *Kluwer: Wireless Personal Communications*, vol. 11, no. 1, pp. 109-129, Oct. 1999.

[13] K. I. Pedersen and P. E. Mogensen, "Simulation of dual-polarized propagation environments for adaptive antennas," in *Proc. IEEE VTC-Fall*, Sep. 1999, pp. 62-66.

[14] R. G. Vaughan, "Signals in mobile communications: A review," *IEEE Trans. Veh. Technol.*, vol. 35, no. 4, pp. 133-145, Nov. 1986.

[15] COST 207 Management Committee, *COST 207: Digital Land Mobile Radio Communications (Final Report)*, Commission of the European Communities, 1989.

[16] GSM Technical Specification, Digital Cellular Telecommunications System; Physical Layer on the Radio Path; General Description (GSM 05.01), ETSI 1997.

[17] G. L. Turin, F. D. Clapp, T. L. Johnston, S. B. Fine, and D. Lavry, "A statistical model of urban multipath propagation," *IEEE Trans. Veh. Technol.*, vol. 21, no. 1, pp. 1-9, Feb. 1972.

[18] A. A. M. Saleh and R. A. Valenzuela, "A statistical model for indoor multipath propagation," *IEEE J. Select. Areas Commun.*, vol. 5, no. 2, pp. 128-137, Feb. 1987.

[19] H. Iwai and Y. Karasawa, "Wideband propagation model for the analysis of the effect of the multipath fading on the near-far problem in CDMA mobile radio systems," *IEICE Trans. Commun.*, vol. 76-B, no. 2, pp. 342-354, Feb. 1993.

[20] M. Hata, "Empirical formula for propagation loss in land mobile radio services," *IEEE Trans. Veh. Technol.*, vol. 29, no. 3, pp. 317-325, Aug. 1980.

[21] J. Walfisch and H. L. Bertoni, "A theoretical model of UHF propagation in urban environments," *IEEE Trans. Antennas Propagat.*, vol. 36, no. 12, pp. 1788-1796, Dec. 1988.

[22] E. Damosso, ed., *Digital Mobile Radio Towards Future Generation Systems, COST 231 Final Report*, EUR 18957, 1999.

[23] F. Ikegami, S. Yoshida, and M. Umehira, "Propagation factors controlling mean field strength on urban streets," *IEEE Trans. Antennas Propagat.,* vol. 32, no. 8, pp. 822-829, Aug. 1984.

[24] F. Dosière, G. Maral, and J.-P. Boutes, "Shadowing process for mobile and personal satellite systems," in *Proc. IEEE Globecom*, Nov. 1995, pp. 536-540.

[25] S. Mockford, A. M. D. Turkmani, and J. D. Parsons, "Local mean signal variability in rural areas at 900 MHz," in *Proc. IEEE VTC*, May 1990, pp. 610-615.

[26] A. Mawira, "Models for the spatial cross-correlation functions of the (log)-normal component of the variability of VHF/UHF field strength in urban environment," in *Proc. IEEE PIMRC*, Oct. 1992, pp. 436-440.

[27] M. Gudmundson, "Correlation model for shadow fading in mobile radio systems," *IEE Electron. Lett.*, vol. 27, no. 3, pp. 2145-2146, Nov. 1991.

[28] T. B. Sørensen, "Correlation model for slow fading in a small urban macro cell," in *Proc. IEEE PIMRC*, Sep. 1998, pp. 1161-1165.

[29] L. J. Greenstein, V. Erceg, Y. S. Yeh, and M. V. Clark, "A new path-gain/delay-spread propagation model for digital cellular channels," *IEEE Trans. Veh. Technol.*, vol. 46, no. 2, pp. 477-485, May 1997.

[30] R. H. Clarke, "A statistical theory of mobile radio reception," *Bell System Technical J.*, vol. 47, pp. 957-1000, July 1968.

[31] K. Kalliola, J. Laurila, M. Toeltsch, K. Hugl, P. Vainikainen, and E. Bonek, "3-D directional wideband dual-polarized measurement of urban mobile radio channel with synthetic aperture technique," in *Proc. AP2000*, Apr. 2000.

[32] H. Asplund and J.-E. Berg, "Estimation of scatterer locations from urban array channel measurements at 1800 MHz," in *Proc. RadioVetenskap och Kommunikation*, June 1999, pp. 136-140.

[33] U. Martin, "A directional radio channel model for densely built-up urban areas," in *Proc. EPMCC*, Oct. 1997, pp. 237-244.

[34] K. I. Pedersen, P. E. Mogensen, and B. H. Fleury, "A stochastic model of temporal and azimuthal dispersion seen at the base station in outdoor propagation environments," *IEEE Trans. Veh. Technol.*, vol. 49, no. 2, pp. 437-447, Mar. 2000.

[35] F. Adachi, M. T. Feeney, A. G. Williamson, and J. D. Parsons, "Cross-correlation between the envelopes of 900 MHz signals received at a mobile radio base station site," *IEE Proc.*, vol. 133, no. 6, pp. 506-512, Oct. 1986.

[36] K. I. Pedersen, P. E. Mogensen, and B. Fleury, "Power azimuth spectrum in outdoor environments," *IEE Electron. Lett.*, vol. 33, no. 18, pp. 1583-1584, Aug. 1997.

[37] T.-S. Chu and L. J. Greenstein, "A semi-empirical representation of antenna diversity gain at cellular and PCS base stations," *IEEE Trans. Commun.*, vol. 45, no. 6, pp. 644-646, June 1997.

[38] K. I. Pedersen, P. E. Mogensen, and B. H. Fleury, "Spatial channel characteristics in outdoor environments and their impact on BS antenna system performance," in *Proc. IEEE VTC*, May 1998, pp. 719-723.

[39] P. Pajusco, "Experimental characterization of D.O.A at the base station in rural and urban area," in *Proc. IEEE VTC*, May 1998, pp. 993-998.

[40] M. Nilsson, B. Lindmark, M. Ahlberg, M. Larsson, and C. Beckman, "Characterization of a wideband radio channel using spatio temporal polarization measurements," in *Proc. IEEE PIMRC*, Sep. 1999, pp. 1278-1283.

[41] M. Pettersen, P. H. Lehne, J. Noll, O. Røstbakken, E. Antonsen, and R. Eckhoff, "Characterisation of the directional wideband radio channel in urban and suburban areas," in *Proc. IEEE VTC-Fall*, Sep. 1999, pp. 1454-1459.

[42] P. E. Mogensen, K. I. Pedersen, P. Leth-Espensen, B. Fleury, F. Frederiksen. K. Olesen, and S. L. Larsen, "Preliminary measurement results from an adaptive antenna array testbed for GSM/UMTS," in *Proc. IEEE VTC*, May 1997, pp. 1592-1596.

[43] C. Chang, H. L. Bertoni, and G. Liang, "Monte Carlo simulation of delay and angle spread in different building environments," in *Proc. IEEE VTC-Fall*, Sep. 2000, pp. 49-56.

[44] K. I. Pedersen, P. E. Mogensen, and B. H. Fleury, "Dual-polarized model of outdoor propagation environments for adaptive antennas," in *Proc. IEEE VTC-Spring*, May 1999, pp. 990-995.

[45] A. A. Glazunov, H. Asplund, and J.-E. Berg, "Statistical analysis of measured short-term impulse response functions of 1.88 GHz radio channels in Stockholm with corresponding channel model," in *Proc. IEEE VTC-Fall*, Sep. 1999, pp. 107-111.

[46] P. C. F. Eggers, J. Toftgård, and A. M. Oprea, "Antenna systems for base station diversity in urban small and micro cells," *IEEE J. Select. Areas Commun.*, vol. 11, no. 7, pp. 1046-1057, Sep. 1993.

[47] Y. Ebine, T. Takahashi, and Y. Tamada, "A study of vertical space diversity for a land mobile radio," *Electron. and Commun. in Japan*, Part I, vol. 74, no. 10, pp. 68-76, 1991.

[48] S. Lundgren and M. Robertsson, "The Crosscorrelation Between 1800 MHz Signal Envelopes Received by Vertically Separated Base Station Antennas." Master's thesis, Royal Institute of Technology, Stockholm, Sweden, May 1995.

[49] A. M. D. Turkmani, A. A. Arowojolu, P. A. Jefford, and C. J. Kellet, "An experimental evaluation of the performance of two-branch space and polarization diversity schemes at 1800 MHz," *IEEE Trans. Veh. Technol.*, vol. 44, no. 2, pp. 318-326, May 1995.

[50] W. C. Y. Lee and Y. S. Yeh, "Polarization diversity system for mobile radio," *IEEE Trans. Commun.*, vol. 20, no. 5, pp. 912-923, Oct. 1972.

[51] F. Lotse, J.-E. Berg, U. Forssén, and P. Idahl, "Base station polarization diversity reception in macrocellular systems at 1800 MHz," in *Proc. IEEE VTC*, May 1996, pp. 1643-1646.

[52] T. B. Sørensen, A. Ø. Nielsen, P. E. Mogensen, M. Tolstrup, and K. Steffensen, "Performance of two-branch polarisation antenna diversity in an operational GSM network," in *Proc. IEEE VTC*, May 1998, pp. 741-746.

[53] S. Kozono, T. Tsuruhara, and M. Sakamoto, "Base station polarization diversity reception for mobile radio," *IEEE Trans. Veh. Technol.*, vol. 33, no. 4, pp. 301-306, Nov. 1984.

[54] T. Taga, "Analysis for mean effective gain of mobile antennas in land mobile radio environments, " *IEEE Trans. Veh. Technol.*, vol. 39, no. 2, pp. 117-131, May 1990.

[55] A. S. Bajwa and J. D. Parsons, "Small-area characterization of UHF urban and suburban mobile radio propagation," *IEE Proceedings*, vol. 129, no. 2, pp. 102-109, Apr. 1982.

[56] A. Kuchar, J.-P. Rossi, and E. Bonek, "Directional macro-cell channel characterization from urban measurements," *IEEE Trans. Antennas Propagat.*, vol. 48, no. 2, pp. 137-146, Feb. 2000.

[57] L. Melin, M. Rönnlund, and R. Angbratt, "Radio wave propagation-A comparison between 900 MHz and 1800 MHz," in *Proc. IEEE VTC*, May 1993, pp. 250-252.

[58] A. Algans, K. I. Pedersen, and P. E. Mogensen, "Experimental analysis of the joint statistical properties of azimuth spread, delay spread, and shadow fading," *IEEE J. Select. Areas Commun.*, vol. 20, no. 3, pp. 523-531, Apr. 2002.

[59] L. Vuokko, P. Vainikainen, and J. Takada, "Clusterization of measured direction-of-arrival data in an urban macrocellular environment," in *Proc. IEEE PIMRC*, Sep. 2003, pp. 1222-1227.

[60] F. Frederiksen, P. E. Mogensen, K. I. Pedersen, and P. Leth-Espensen, "Testbed for evaluation of adaptive antennas for GSM and wideband-CDMA," in *Proc. COST 252/259 Joint Workshop*, Apr. 1998, pp. 171-181.

[61] H. Hofstetter, A. F. Molisch, and M. Steinbauer, "Implementation of a COST 259 geometry based stochastic channel model for macro- and microcells," in *Proc. EPMCC*, Feb. 2001.

[62] 3rd Generation Partnership Project; Technical Specification Group (TSG) RAN WG4; "Deployment aspects," 3G TR 25.943 V2.0.0 (2000-03).

[63] A. F. Molisch, M. Steinbauer, H. Asplund, and N. B. Mehta, "Backward compatibility of the COST 259 channel model," in *Proc. WPMC*, Oct. 2002, pp. 549-553.

[64] L. J. Greenstein, D. G. Michelson, and V. Erceg, "Moment-method estimation of the Ricean *K*-Factor," *IEEE Commun. Lett.*, vol. 3, no. 6, pp. 175-176, June 1999.

ACKNOWLEDGMENTS

The authors wishes to thank the participants of the COST 259 project, especially the members of the channel modeling sub-working group, for their valuable input in developing the channel model. The input of the anonymous reviewers has also improved the quality of the paper. We are especially grateful to Dr. Robert Bultitude, whose detailed and constructive suggestions contributed enormously to this paper.

Henrik Asplund (M'05) received the M.Sc. degree from Uppsala University, Sweden in 1996. Since then he has been with the Antenna Systems and Propagation Research Group at Ericsson Research, Stockholm, Sweden. His

current research interests are measurement and modeling of mobile radio channels, antenna diversity, smart antennas, and MIMO systems. Henrik Asplund has participated in the European research initiatives "COST 259" and "COST 273."

Andrés Alayón Glazunov was born in Havana, Cuba, in 1969. He obtained his M.Sc. (Engineer-Researcher) degree from Saint Petersburg's State Technical University, Russia, in 1994, in Physical Engineering with specialization in Physical Electronics. From 1996 to 2001, he was a Member of the Research Staff at Ericsson Research, Ericsson AB in Kista, Sweden, where he conducted research in the areas of RAKE receiver performance evaluation for UMTS, applied electromagnetic wave propagation and stochastic channel modelling for wireless communications systems. During this period he contributed to the European COST Action 259 project in the directional channel modelling working group. In 2001, Alayón Glazunov joined Telia Research, Sweden, where he first held a Senior Research Engineer position. Later, starting 2003, he held a position as Senior Specialist in Antenna Systems and Propagation at TeliaSonera Sweden, where he pursued research in smart antennas, network optimization and handset antenna efficiency measurements and evaluation of their impact on wireless network performance. From 2001 to 2005 he was the Swedish delegate to the European COST Action 273 and was active in the handset antenna working group. He has also contributed to and co-edited the COST273 technical report, upon which the 3GPP standard for measurements of radio performances for UMTS terminals is currently being agreed. Alayón Glazunov has contributed to the EVEREST and NEWCOM European research projects and to both the 3GPP and the ITU standardization bodies. Since June 2006 Alayón Glazunov is a full-time Ph.D. candidate at the Electroscience Dept., Lund University, Sweden. His current research interest is focused on the interaction between the antennas and the radio propagation channel for MIMO wireless systems.

Andreas Molisch (S'89-M'95-SM'00-F'05) received the Dipl. Ing., Dr. techn., and habilitation degrees from the Technical University Vienna (Austria) in 1990, 1994, and 1999, respectively. From 1991 to 2000, he was with the TU Vienna, becoming an associate professor there in 1999. From 2000-2002, he was with the Wireless Systems Research Department at AT&T (Bell) Laboratories Research in Middletown, NJ. Since then, he has been with Mitsubishi Electric Research Labs, Cambridge, MA, USA, where he is a Distinguished Member of Technical Staff. He is also professor and chairholder for radio systems at Lund University, Sweden.

Dr. Molisch has done research in the areas of SAW filters, radiative transfer in atomic vapors, atomic line filters, smart antennas, and wideband systems. His current research interests are MIMO systems, measurement and modeling of mobile radio channels, and UWB. Dr. Molisch has authored, co-authored or edited four books (among them the recent textbook *Wireless Communications*, Wiley-IEEE Press), eleven book chapters, ninety-five journal papers, and numerous conference contributions.

Dr. Molisch is an editor of the IEEE TRANS. WIRELESS COMM., co-editor of a recent special issue on MIMO and smart antennas in J. Wireless Comm. Mob. Comp., and co-editor of a recent JSAC special issue on UWB. He has been member of numerous TPCs, vice chair of the TPC of VTC 2005 spring, and will be general chair of ICUWB 2006. He has participated in the European research initiatives "COST 231," "COST 259," and "COST273," where he was chairman of the MIMO channel working group, and is also chairman of Commission C (signals and systems) of URSI (International Union of Radio Scientists). Dr. Molisch is a Fellow of the IEEE and recipient of several awards.

Klaus Ingeman Pedersen (S'97) received his M.Sc. E.E. and Ph.D. degrees in 1996 and 2000 from Aalborg University, Denmark. His contribution to this paper originates from his Ph.D. studies at Aalborg University. He is currently with Nokia Networks in Aalborg, Denmark. His primary interest is radio resource management and network level performance evaluation for 3G and UTRAN long term evolution.

Martin Steinbauer (S'99-M'02) received his Dipl.-Ing. (1996) and Doctoral Degree (2001), both with distinction, from Vienna University of Technology, Austria (TU-Wien). He received two performance scholarships. After his diploma thesis which he conducted for the German mobile network operator E-Plus GmbH., Düsseldorf, he was research assistant at the Institute of Communications and Radio Frequency Engineering at TU-Wien. From 2002 to first half of 2005 he was with the Network Planning division at mobilkom austria AG&CoKG, Vienna. In 2005, he joined the Group Technology division within mobilkom austria group services GmbH.

Dr. Steinbauer has done research in the field of mobile radio measurement and modeling for simulation, wideband non-stationary channel characterization, clustering effects, and signal processing for MIMO channel estimation. He did pioneer work in MIMO measurements that he conducted together with TU-Ilmenau. Dr. Steinbauer participated in the EU projekt METAMORP and was chairman of the subworking group on directional channel modeling within the European research initiative COST259. He authored or co-authored several publications in the field of mobile radio.